C. V. Robinson and J. T. S. Hopper

DOI: 10.1002/anie.201403741

Protein Interactions

Mass Spectrometry Quantifies Protein Interactions—From Molecular Chaperones to Membrane Porins

*Jonathan T. S. Hopper and Carol V. Robinson**

Keywords:
binding constants · ion mobility · mass spectrometry · membrane proteins · protein–protein interactions

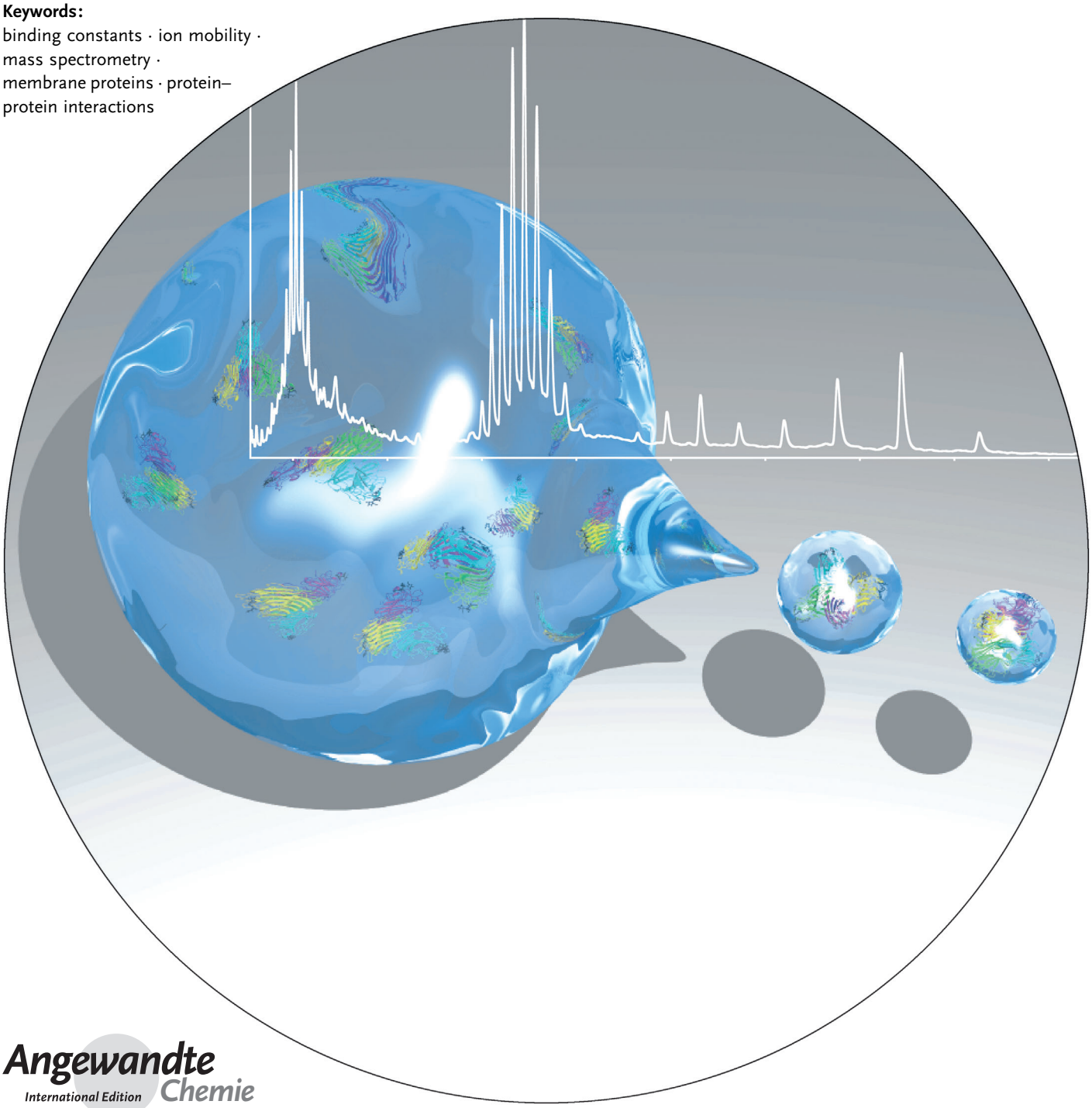

Angewandte International Edition Chemie

Proteins possess an intimate relationship between their structure and function, with folded protein structures generating recognition motifs for the binding of ligands and other proteins. Mass spectrometry (MS) can provide information on a number of levels of protein structure, from the primary amino acid sequence to its three-dimensional fold and quaternary interactions. Given that MS is a gas-phase technique, with its foundations in analytical chemistry, it is perhaps counter-intuitive to use it to study the structure and non-covalent interactions of proteins that form in solution. Herein we show, however, that MS can go beyond simply preserving protein interactions in the gas phase by providing new insight into dynamic interaction networks, dissociation mechanisms, and the cooperativity of ligand binding. We consider potential pitfalls in data interpretation and place particular emphasis on recent studies that revealed quantitative information about dynamic protein interactions, in both soluble and membrane-embedded assemblies.

From the Contents

1. Introduction

Understanding the interactome, the complete set of protein interactions in a cell, is a formidable task that has become a vital part of the proteomic effort.[1] Not only is the number of interactions almost incomprehensible but the networks are dynamic and change in response to various stimuli.[2] Furthermore, some interactions are transient, and detecting these short-lived interactions without perturbing their equilibrium is problematic. An important aspect of describing a particular interaction is to obtain quantitative data for binding affinities. This information, when coupled with cellular concentrations of proteins and ligands, enables the prediction of the dynamic interactome and provides the missing link to systems biology.[3] To achieve this reliable numerical values are required, specifically dissociation constants (K_D), which define the strengths of the interactions. How best to monitor binding events and hence deduce these K_D values for two proteins, or between a protein and its cognate ligand, is a challenge that has spawned over 20 biophysical techniques.[4]

The biophysical techniques that have been developed to study dissociation constants can be categorized as either "separative" or "non-separative" methods. The former rely on separating and quantifying individual components of an interaction, using techniques such as liquid chromatography[5] and capillary electrophoresis.[6] The non-separative approaches, for example, calorimetric techniques, rely on their ability to measure a change in a physical property in response to binding. Measuring heat changes that are associated with an interaction between two species forms the basis of isothermal titration calorimetry (ITC). Similarly, spectroscopic techniques, such as fluorescence anisotropy (FA), surface plasmon resonance (SPR), and NMR spectroscopy, are non-separative and yield discrete changes upon binding. Detecting the increase in mass or size induced by binding is perhaps the most direct way to measure physical change without separation. This property is exploited in solution-based methods, such as analytical ultracentrifugation (AUC) and dynamic light scattering (DLS).

1.1 Evolution of Mass Spectrometry for Biomolecular Analysis

Mass spectrometry (MS) is a relative newcomer to the study of protein interactions, primarily because until a few decades ago, the technique was limited to relatively low-molecular-mass volatile molecules. Biomolecular MS evolved from pioneering developments in soft ionization techniques.[7] Specifically, electrospray ionization (ESI) overcame the limitations associated with generating gas-phase ions from involatile species. A nanoflow adaptation of ESI, nanoESI (nESI), possesses notable advantages for analyzing large protein assemblies, which include increased sensitivity, better tolerance to salts, and more efficient desolvation, removing the requirement for drying gases and heating to evaporate the solvents.[8] The most notable characteristic associated with ESI or nESI, which is pertinent to this Review, is the ability to preserve weak non-covalent interactions between protein subunits and ligands that exist in solution.[9]

[*] Dr. J. T. S. Hopper, Prof. Dr. C. V. Robinson
Physical and Theoretical Chemistry Laboratory
University of Oxford
South Parks Road, Oxford OX1 3QZ (UK)
E-mail: carol.robinson@chem.ox.ac.uk

Careful transfer from solution to the gas phase enables extremely large and intricate assemblies to be projected intact into the mass spectrometer. Transmission of high m/z ions is greatly improved by means of increased pressures within the instrument,[10] which focuses the ions and dissipates their excess kinetic energy through collisions with residual gas molecules (collisional focusing).[11] Lowering the radio frequencies of the quadrupole analyzer to 300 kHz extends the accessible m/z range to 32400.[10] These modifications have allowed large biomolecular assemblies, including ribosomes,[12] proteasomes,[13] and virus capsids of approximately 18 MDa,[14] to be transmitted intact within the mass spectrometer. In theory, mass spectrometry is therefore capable of providing a platform for monitoring the formation of noncovalent interactions in a wide range of macromolecular assemblies, from single ligands and proteins through to macromolecular assemblies of MDa proportions.[15]

Although the detection of protein assemblies is performed in the gas phase, the process essentially allows a snapshot of the binding equilibrium established in solution to be captured and detected in the mass spectrometer. Two types of experiments are possible: either controlling the concentration of the binding partners or limiting their interaction time. Binding affinities are obtained from concentration-controlled experiments wherein the binding partners are incubated in solution at different ratios, and mass spectra are recorded once an equilibrium has been established, following a constant incubation time. Kinetic information is derived from time-dependent studies wherein binding partners are incubated, aliquots removed, and mass spectra recorded after specified time intervals. Ideally, the concentrations of the various protein–ligand systems in both types of experiment should be close to those that are physiologically relevant. Given the unevenness in local concentrations within cells however, as a result of molecular crowding, nanomolar through to millimolar protein concentrations should be explored to encapsulate the full range of binding interactions.

For time-resolved experiments, the life time of transient interactions can pose a significant problem for their capture by most biophysical approaches. Since the complexes that are formed are short-lived and will only be present at low concentrations, these transient events can sometimes be trapped by MS analysis as the time from desolvation/ionization to recording a spectrum is typically tens or hundreds of milliseconds. Such a timeframe therefore enables binding events to be monitored in real time (see Section 3).[16] Both time-resolved and concentration-dependent MS investigations will be considered in this Review (Figure 1).

One of the great advantages of MS in the study of biomolecular interactions is sensitivity. Typically, picomolar amounts of a protein complex are required. In contrast, ITC or NMR spectroscopy generally require millimolar amounts of a protein. Even the most sensitive ITC equipment requires at least three orders of magnitude more protein complex than MS. Although SPR and FA compete in terms of sensitivity they are not capable of measuring interactions between unmodified protein ligands that exist freely in solution. For SPR, one of the binding partners must be immobilized onto a surface. This tethering can in some cases lead to a loss in activity or avidity effects.[17] The requirement to fluorescently label one species in FA measurements also raises concerns about the effects of labelled ligands on the receptor binding properties.

For most biophysical methods, a wide range of buffers can be used. A major limitation of the ESI technique, however, is its intolerance to the non-volatile buffer salts that are used in molecular-biology protocols. Many samples therefore require desalting before analysis, and buffers such as ammonium acetate are preferred as they are easily removed during the desolvation process. The range of concentrations amenable to ESI-MS studies will also impose restrictions on the range of affinities that can be measured using this technique, which is discussed in more detail in Section 4.

A further consideration is the ability of MS to simultaneously detect all species present in a given solution based on the dynamic range and mass resolution provided by the technique. These characteristics, as well as the rapid timeframe on which measurements can be made, make MS highly valuable for studying interactions that form with ligands to allow reaction to occur or transient oligomeric states, since these can be visualized among other, more abundant species. This is particularly important for the complex interaction networks that exist in equilibrium as distinct species can be visualized simultaneously without having to isolate specific complexes, which would inevitably perturb the equilibrium. This ability to detect complexes simultaneously is particularly important for studying the subunit exchange of protein complexes as multiple products can be resolved/separated according to their mass. Subunit exchange has been monitored by means of other techniques, such as ion exchange chromatography and fluorescence resonance energy transfer (FRET). Although FRET possesses a distinct advantage over

Jonathan T. S. Hopper obtained his B.Sc. in chemistry at the University of Sheffield and an M.Sc. in analytical chemistry at Loughborough University. He subsequently moved to the University of Nottingham where he gained a Ph.D. in biomolecular mass spectrometry under the supervision of Dr. Neil Oldham. He moved to the University of Oxford to work with Professor Robinson on the application of mass spectrometry to intact membrane protein assemblies.

Carol V. Robinson obtained her Ph.D. studying under the supervision of Prof. Dudley Williams at the University of Cambridge. Her research career spans some 20 years and has focused primarily on defining folding and binding of proteins and their cognate ligands. Recently her group has developed novel approaches to project membrane protein complexes into the gas phase of the mass spectrometer where they can be interrogated for their lipid- and drug-binding properties.

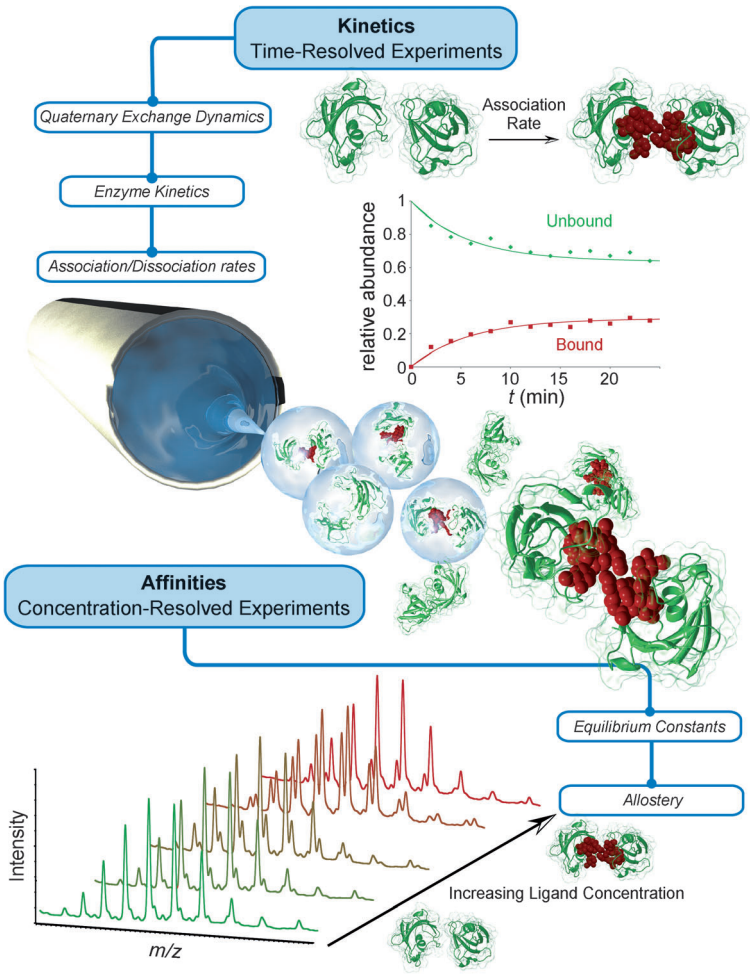

Figure 1. An overview of the experimental approaches discussed within this Review and the information that can be extracted. A time-resolved experiment (upper panel) in which the formation of the bound complex (red) is monitored over time, enabling association rates to be calculated. Measurements performed at equilibrium (lower panel) where the concentration of one component, in this case the ligand, is increased systematically. The populations of different species are then plotted as a function of ligand concentration to allow interaction affinities to be determined.

many techniques by being applicable in vivo, both techniques require the labelling of protein subunits and hence are prone to disadvantages similar to those discussed above for SPR and FA. For MS experiments, the opportunity to use isotopically labelled (e.g., ^{15}N-labelled) proteins avoids the potentially deleterious effects of a tag.

A further attribute of the MS method is the additional information available on the folded state of a protein or complex upon binding. This information is contained within the charge state series, a direct relationship between the surface area available for protonation and the charge states observed in a mass spectrum.[18] As decreases in the surface area can be brought about by forming protein interfaces, or by folding, an indication of conformational change upon binding can be attained.

In this Review, we present recent highlights that exploit the ability of MS to detect protein interactions in solution. In all cases, these applications benefit from the ability to quantify the affinity of protein interactions at equilibrium and to study exchange kinetics in multi-protein assemblies. We also highlight applications to monitor enzymatic reactions and to understand the allosteric communication of multiple ligands that interact at separate interfaces of a protein complex.

2. Snapshots of Protein Complexes at Equilibrium

The introduction of a protein and its cognate ligand into the MS allows a "snapshot" of the interactions formed in solution at a particular point in time to be captured. Mass spectra recorded for solutions at equilibrium allow direct access to the dissociation constants of an interaction by assessing the intensities of the peak corresponding to the protein–ligand complex, relative to that corresponding to the apo protein. Knowledge of the initial concentrations in the individual solutions is crucial in enabling the calculation of dissociation constants (K_D). Typically, experiments are performed over a range of protein or ligand concentrations and analyzed by one of two mathematical frameworks. The first method calculates the association constant at each concentration and averages these values.[19] The second fits the data using a non-linear function.[20] Both approaches have been applied to study protein interactions with fatty acids[21] and carbohydrates.[22]

A particularly powerful example of binding affinity determination was recently reported for noroviruses, a group of viral pathogens that are responsible for acute gastroenteritis and recognize the human histo-blood group antigens (HBGA).[23] The C-terminal protrusion domain (P) of the major capsid protein forms the exterior of the capsid and is responsible for the interaction with the HBGAs. The affinities of 41 HBGAs for dimers of the P protein were quantified and found to range from 400 to 3000 M^{-1}. These measurements therefore enabled a correlation to be established between chain type and affinity.[24]

Variations to time-resolved and concentration-dependent experiments have expanded the application of MS to increasingly complex systems in which ligands are difficult to resolve. As large assemblies typically undergo less efficient desolvation within the mass spectrometer, resulting in broad peak widths,[12] the binding of low-molecular-weight ligands is often concealed. By including a proxy protein (P_{proxy}) of low molecular mass that interacts specifically with the ligand of interest, it is possible to measure quantitatively the extent of ligand binding to large assemblies. This approach was applied to determine the interactions between a range of oligosaccharides and the homotrimeric tailspike protein of the bacteriophage P22.[25] A 27 kDa single-chain antibody acted as P_{proxy} binding to ligands with predetermined affinities. The fraction of the P_{proxy}/ligand complex responds in real time to

changes in the ligand concentration and therefore can be used to report on the fraction of ligand bound to the tailspike protein. The affinity measurements obtained by MS corroborated K_a values determined previously by means of a fluorescence-quenching assay.

An alternative strategy to address the problem of unresolved ligand binding in larger complexes is termed "catch and release". As its name suggests, the approach involves releasing ligands from protein complexes and is carried out in the gas phase using collision-induced dissociation (CID). The mass of the ligand released in this step can be determined and subjected to further fragmentation to confirm its identity. A recent study investigated the potential of this technique by incubating target proteins, either a single-chain antibody, an antigen-binding fragment, or a fragment of a bacterial toxin, with a library of potential carbohydrate binding partners.[26] A library of over 200 carbohydrates was screened with multiple protein targets to identify ligands that bind with affinities in the range of 10^3 to $10^6\,\text{M}^{-1}$.

An interesting development of this catch-and-release approach was its combination with ion mobility (IM) spectrometry, a gas-phase electrophoretic technique that enables separation based on drift velocity through a buffer gas and is therefore dependent on charge, size, and shape.[27] By combining these two methods structural isomers of carbohydrate ligands that were released from monoclonal antibody fragments were identified.[28] Libraries of carbohydrates have also been subjected to screening using the catch-and-release method to identify interactions with the norovirus particle of VA387.[22a] Interactions were detected with all human histo-blood group antigens (HBGAs) that had previously been shown to be norovirus receptors, together with a number of new interactions with oligosaccharides present in the cell wall of mycobacteria and human milk.

3. Monitoring the Formation of Protein Assemblies in Real Time

As a network of interactions forms and dissipates, it is possible to monitor this dynamic process in real time. Experimentally, this requires determination of the population of the bound protein, relative to that of the unbound protein, as a function of time. Data is then analyzed by optimizing the on/off rates to achieve the best fit with the experimental data, which has been described in detail elsewhere.[29] For reactions where time points are taken at intervals of minutes or more, this is achieved by incubating proteins and ligands off-line and by recording spectra at predetermined time points. For rapid reactions, where second/millisecond reaction times are of interest, protein and ligand can be infused from separate syringes and mixed using a T-piece at short timeframes prior to electrospray ionization. When applied to protein folding experiments, the structural information that is obtained from the charge state signatures or extracted by IM–MS allows conformational transitions to be probed. Early applications include the real-time monitoring of the folding of cytochrome c,[30] as well as the unfolding of myoglobin.[31] Unlike the unfolding of apo-myoglobin, which is non-cooperative, holo-myoglobin moves between defined conformational states in a cooperative unfolding pathway. Using this MS approach, a novel intermediate was observed, with an unperturbed chromophore within the heme binding pocket. This intermediate had, however, undergone partial unfolding, which was revealed by shifts in the charge state distribution and interestingly had not been detected previously by optical spectroscopy, highlighting the sensitivity of this MS method.

Using similar real-time unfolding experiments, the heme binding states of hemoglobin were monitored by denaturation in solution followed by dialysis into refolding buffer.[32] Aliquots were taken at specified refolding time points and analyzed by MS. On refolding, the alpha and beta subunits were able to reinstate intermolecular interactions between the protein subunits as well as with the heme. The assembly pathway that was determined involved heme-bound monomers that proceeded to heterodimers; ultimately, heterodimer association resulted in native tetrameric hemoglobin.

Analogous experiments added detail to the catalytic mechanism of the enzyme 3-deoxy-d-manno-2-octulosonate-8-phosphate synthase (KDO8PS), which is responsible for the biosynthesis of lipopolysaccharides.[33] A new reaction intermediate that was bound to the enzyme was identified. This intermediate had not been observed previously owing to its dynamic nature. The continuous-flow approach, which is capable of sampling on the millisecond time range, has recently been coupled with desorption electrospray ionization (DESI) to allow reaction monitoring with a time resolution of as low as a 300 μs.[34]

4. Implications of the Phase Transition

The use of MS to quantify the affinity/kinetics of protein interactions is built upon the premise that spectra are able to provide an accurate representation of the degree of binding in solution. In order to extract affinity data, as described in Sections 2 and 3, the ratio between peaks that result from bound and unbound protein is monitored as a function of concentration or time. Concerns arise from effects that may perturb this ratio. Of particular concern has been the desolvation process that could result in radical concentration changes within the ES droplets, which could distort the equilibria. This concern is partially alleviated for the smaller droplets generated in nESI as desolvation is much faster than the kinetic rate of forming new interactions, which could perturb the equilibrium. This is especially true for large ligands, particularly proteins, with correspondingly lower diffusion coefficients than smaller ligands.[35] For small ligands, any unbound material should be ejected from the droplets before complete desolvation, as small molecules are expected to be ionized according to the ion evaporation model.[36] Strong experimental evidence for the retention of the status of a dynamic equilibrium was gleaned from an MS study of small heat shock proteins, which exist in a range of interconverting oligomeric states. A direct comparison of the oligomeric distribution observed by MS and size-exclusion chromatography multi-angle light scattering (SEC–MALS) revealed excellent agreement between the solution- and gas-

phase measurements (Figure 2a) and supports the idea that the equilibria are not perturbed during the phase transition, at least for large protein assemblies.[37]

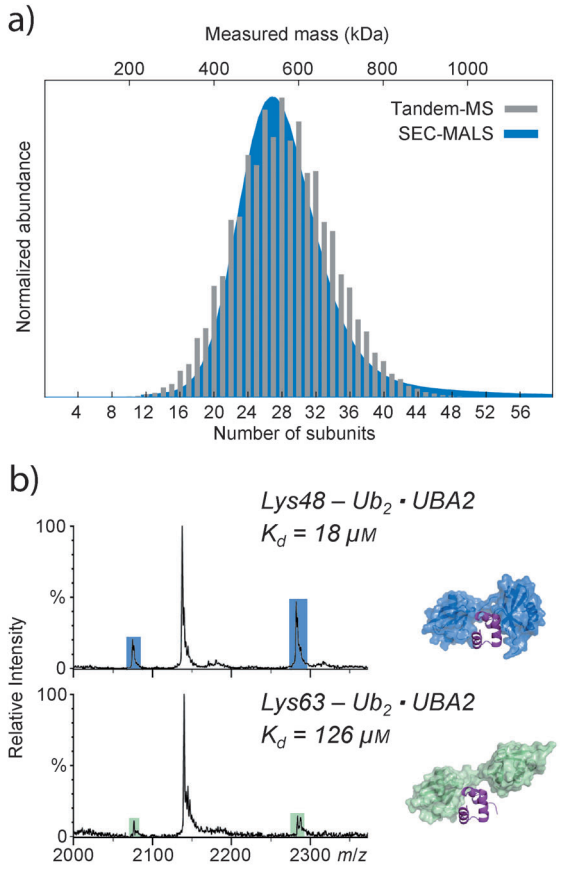

Figure 2. a) The distribution of oligomers observed using MS (gray bars) closely reflects the distribution present in solution, which was characterized using SEC–MALS (blue trace). b) ESI–MS conditions optimized using charge reduction to allow the preservation of weak di-ubiquitin–UBA2 interactions. The higher degree of binding in the upper spectrum illustrates the higher specificity of Lys-48 linked ubiquitin for this domain relative to the Lys-63 topology in the lower spectrum. Figure adapted from Ref. [37] and [41].

Related to these concerns is the possibility that two species that were originally not associated in the bulk solution become encapsulated in the same final droplet (or final solvation shell) prior to ionization. In such a circumstance, the two species become associated following the removal of the last remaining water molecules. The contribution of this effect is strongly related to the concentration of the species in solution and can be mitigated by working at low protein/ligand concentrations (low μM range). Moreover, non-specific interactions that form during the rapid desolvation process are not expected to form in the correct orientation in the correct binding pocket. The interactions formed on the surface of a protein will lead to a complex that is notably weaker than the specific interactions formed at equilibrium and could potentially readily dissociate following desolvation.[35] When studying low-affinity interactions, which necessitate high concentrations of proteins and ligands, statistical treatments can be applied to account for non-specific interactions that arise during the ESI process.[38] Arguably the most promising method for determining the presence of non-specific interactions is to include a reference protein that does not interact with the ligand under investigation.[39] Non-specific binding with the reference protein, as well as with the target protein, can therefore be taken into account in the calculation of the binding affinities.

Differences in the ionization efficiency, transmission, and detector response of bound and unbound counterparts should also be considered as factors that could influence results. It was recently demonstrated that the presence of virus capsids in the same solution reduced the extent of binding observed between a single-chain variable fragment (scFv) of a monoclonal antibody and an octasaccharide ligand.[40] It was proposed that the observed effect was due to a reduction in the amount of available surface in the electrospray droplet. The protein and the protein–ligand complex must therefore compete with each other for surface accessibility, which is reduced owing to the presence of the virus capsid. In this case, the free protein, which is more hydrophobic, outcompetes the more hydrophilic P–L complex for available surface sites. These different surface properties were proposed to explain the change in ionization efficiency (and therefore, the ratio observed).

As a general rule it has been suggested that ligand binding that results in $<10\,\%$ increase in mass relative to the protein alone does not cause significant differences in ionization efficiency, transmission, and detection.[19] Recent applications to protein–protein complexes, such as ubiquitin–ubiquitin binding domain interactions[41] and the HSP90 reaction cycle,[29] in which significant changes in mass accompany the binding event, demonstrate that this $<10\,\%$ rule is not universally applicable.

The dissociation of a protein complex after nESI, but prior to detection is perhaps the most fundamental concern for MS studies of protein complexes. If dissociation occurs, it will lead to an overestimation of the K_D value. This was initially a fundamental concern for protein–ligand interactions that rely heavily on hydrophobic interactions, which are discussed in Section 5.[42] Methods that minimize the charge acquired by complexes during ionization can reduce unwanted dissociation by decreasing the kinetic energy and thereby minimizing the energy gained from subsequent collisions. The use of imidazole,[43] the addition of basic solvents to protein-containing solutions, and the introduction of solvent vapors to the source housing[44] have all enhanced the preservation of weak intermolecular interactions. Significant charge reduction allows the preservation of weak intermolecular interactions, such as those between di-ubiquitin and ubiquitin binding domains (Figure 2b), and reveals the specificity that exists between these different lysine linkages (K48 or K63 linked di-ubiquitin).[41]

5. Survival of Hydrophobic Interactions in a Dehydrated Environment

The effects on protein structure of transferring protein complexes from solution to the desolvated environment of a mass spectrometer have been debated since the first applications of this technique to biomolecules. Fundamental interactions that are responsible for the protein structure are heavily influenced by the shielding effects of water. Generally, these interactions include hydrogen bonds, electrostatic interactions, and van der Waals forces, all of which are increased in the absence of water. A re-occurring concern has been the fate of hydrophobic interactions. However, van der Waals/dispersion forces between hydrophobic contacts must be sufficient to preserve such complexes within the mass spectrometer given the numerous reports of hydrophobic membrane–protein complexes that survive in vacuum.[45]

Considering the associations that are preserved in the gas phase and rely almost exclusively on hydrophobic interactions,[46] a series of studies that focus on the interactions between bovine β-lactoglobulin and a range of fatty acids are particularly impressive.[47] The interaction strengths of these complexes were interrogated using time-resolved blackbody infrared radiative dissociation (BIRD) in the gas phase. The fatty acids feature carboxylic acid groups, which form hydrogen bonds to the protein chain. Interestingly, however, the activation energy required for gas-phase dissociation of the ligand was sensitive to the alkyl chain length, demonstrating that these hydrophobic interactions are preserved in vacuum.[47a] In a similar vein, a series of synthetic supramolecular complexes, which interact with β-cyclodextrins solely through hydrophobic forces, were investigated using a range of ESI variants, including nano-ESI, cold-spray ionization, and electrosonic spray ionization, for their ability to preserve these interactions within the mass spectrometer.[48] As no other interactions were possible in these complexes, the study provided unambiguous evidence that hydrophobic interactions can be preserved in the gas phase.

Having established that hydrophobic interactions between small proteins can survive the electrospray process and gas-phase transmission within the instrument, the affinity and specificity of different poly-Ub chains, which interact through hydrophobic forces, were investigated with a range of ubiquitin-binding domains (UBD).[41] Charge reduction was employed to negate gas-phase dissociation effects (Figure 2b), and the approach was validated using previously characterized Ub–UBD complexes. Interactions with UBDs act to control the fate of the poly-ubiquitin-linked proteins. The Ub-associated domain 2 (UBA2) of HR23a, which mediates the delivery of substrates to the proteasome, displays increased affinity towards K48-linked chains, as corroborated by MS (Figure 2b). The binding affinities for unknown UBD–Ub interactions were also determined, and the detection of a ternary complex, formed between Ub and two different UBDs, suggests the possibility of cross-talk between separate Ub signaling pathways. Interestingly, it was possible to determine K_D values of up to 200 μM for the weakest of the UBD–Ub complexes studied at a near physiological concentration (4 μM of UBD).

A critical point to make before closing this discussion on hydrophobic interactions is that the timeframe of MS measurements, that is, the time that protein complexes exist in a desolvated state before detection, is of the order of a few milliseconds. Consequently, although desolvated protein complexes are unlikely to exist in a conformation that is at an energy minimum, the measurements are performed on a faster timescale than the kinetics of structural rearrangements, implying that metastability is an important factor in their survival.[49]

6. Probing Allostery in Protein Complexes

Allostery refers to an effect whereby the binding of a modulator to a protein induces a response in the complex. This response is transmitted throughout the protein structure to activate the complex towards a subsequent binding event.[50] This can be viewed simplistically as a molecular switch, and such interactions are common regulatory controls within the cell. Unravelling the cooperativity of metal-ion binding to various proteins[51] and deciphering interactions of cofactors binding to glyceraldehyde-3-phosphate dehydrogenase[52] represent allosteric binding mechanisms that were observed using MS. Recently, the homotetrameric enzyme fructose 1,6-bisphosphatase (FBPase), a potential target for diabetes treatment, was studied in combination with a range of inhibitors.[53] A clear enhancement of successive inhibitor binding implies that the four sites act with positive cooperativity.

An impressive study of allosteric binding was demonstrated for GroEL,[54] an 800 kDa molecular chaperonin, which consists of two stacked homoheptameric rings providing 14 ATP binding sites. Folding of the target proteins takes place through ATP-driven allosteric movements of the molecular machine.[55] Given that the mass of ATP amounts to only approximately 0.06% of the mass of GroEL, a key factor of the experimental design was to increase the difference in *m/z* for each ATP binding event. This was achieved by charge reduction using a range of volatile MS-compatible buffers (Figure 3a). Ammonium acetate was avoided as NH_4^+ can substitute for K^+ in promoting ATP hydrolysis by GroEL, leading to heterogeneous spectra. Ethylenediammonium diacetate (EDDA) prevented ATP hydrolysis, and the accompanying charge reduction increased the separation between successive ATP binding events, allowing their abundance to be measured as a function of ATP concentration (Figure 3b,c). Hill coefficients were calculated for different degrees of saturation of the binding sites and allowed the K_D values of subsequent binding events to be calculated. The data provide compelling evidence for the allosteric communication transmitted following successive binding events.

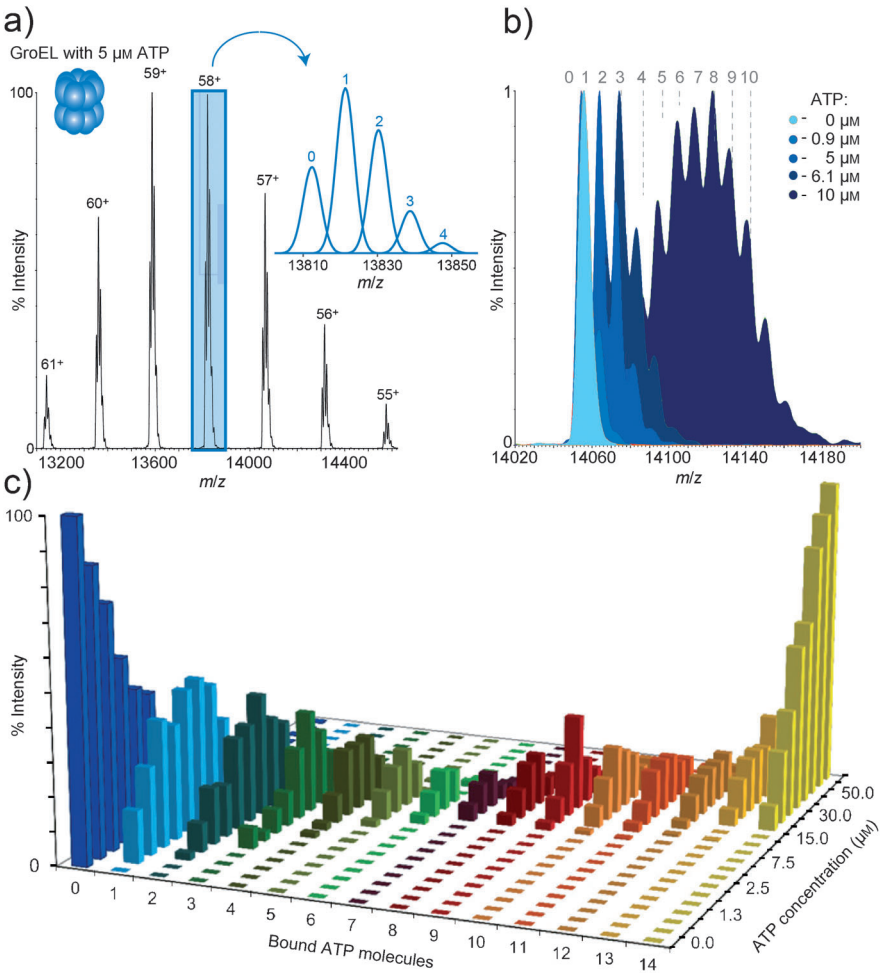

Figure 3. a) Charge-reduced spectra of the GroEL complex for the resolution/separation of the binding of multiple ATP molecules in (b). c) Monitoring the population of each binding event as a function of concentration provides a measure of the affinity, which, in this case, reveals the allosteric communication within the complex. Figure republished with permission from Ref. [54].

7. Unravelling Heterogeneity and Dynamics in Assembly Cycles

The heat shock proteins are up-regulated under conditions of cellular stress, HSP90 being one of the most abundant (1–2 % of the total cellular protein mass).[56] The functional activity of this complex is the result of a highly dynamic and cooperative assembly, which incorporates a variety of co-chaperones. The resulting heterogeneous nature of the complexes formed is challenging for other biophysical techniques mentioned earlier, but has recently been studied using MS.[29] The spectra recorded were difficult to interpret using conventional software, owing to numerous interactions occurring simultaneously leading to many overlapping complexes that had to be deconvoluted using software designed in-house (Figure 4a).[57] Real-time assembly experiments allowed the formation and dissociation of numerous complexes to be monitored simultaneously (Figure 4b). From multiple mass spectra it was possible to calculate 14 K_D values for the equilibria observed by MS. The data also unraveled the specificity of the complex formation, which is summarized along with the K_D values in Figure 4c. Combining K_D values with the cellular concentrations of the individual components allowed the complexes that form within the cell to be defined.

7.1. Quaternary Exchange Dynamics in Protein Assemblies

At equilibrium, some protein complexes exist as polydisperse assemblies, populating a range of oligomeric states, which are often influenced by changes in their environment and represent challenging systems for study by conventional structural biology approaches. The evolution of such dynamic assemblies can only be understood by determining how this behavior promotes their function. Traditional techniques, where data is representative of an average behavior in solution, are not suitable for studying the behavior of a particular oligomeric state. As demonstrated in Section 7 already, a real-time approach can be applied to monitor the quaternary dynamics of polydisperse systems at equilibrium under defined environmental conditions. Subunit exchange experiments rely on the differences in mass between subunits to monitor their incorporation into an assembly. The incorporation of a truncated version of the protein, for example, into an assembly highlights the effect of specific residues on quaternary dynamics. Alternatively, homo-oligomeric assemblies can be studied by monitoring the incorporation of subunits that have been labelled with heavy elements (^{13}C and/or ^{15}N). These methods have been used to characterize the subunit dynamics of IgG antibodies,[58] HBV capsids,[59] and protein cages.[60]

Small heat shock proteins (sHSPs) exist in a range of interconverting oligomeric states,[61] and their primary role is to interact with misfolded proteins to prevent aggregation.[62] Dysfunctions of these proteins are implicated in numerous diseases.[63] Of particular interest are the α-crystallins, mammalian sHSPs that are found in exceptionally high abundance in the eye lens.[64] They populate a range of interconverting oligomeric states with molecular masses ranging from approximately 300 kDa to over 1 MDa. Early subunit-exchange experiments on αA-crystallin explored the contributions of five C-terminal residues by truncating the protein and comparing its behavior with that of the wild-type protein.[65] The truncation reduces the size of the oligomers adopted by the assembly. αB-crystallin, also a component of the α-crystallin assemblies in the eye, was studied in the presence of αA-crystallin. Unlike other sHSPs, the mamma-

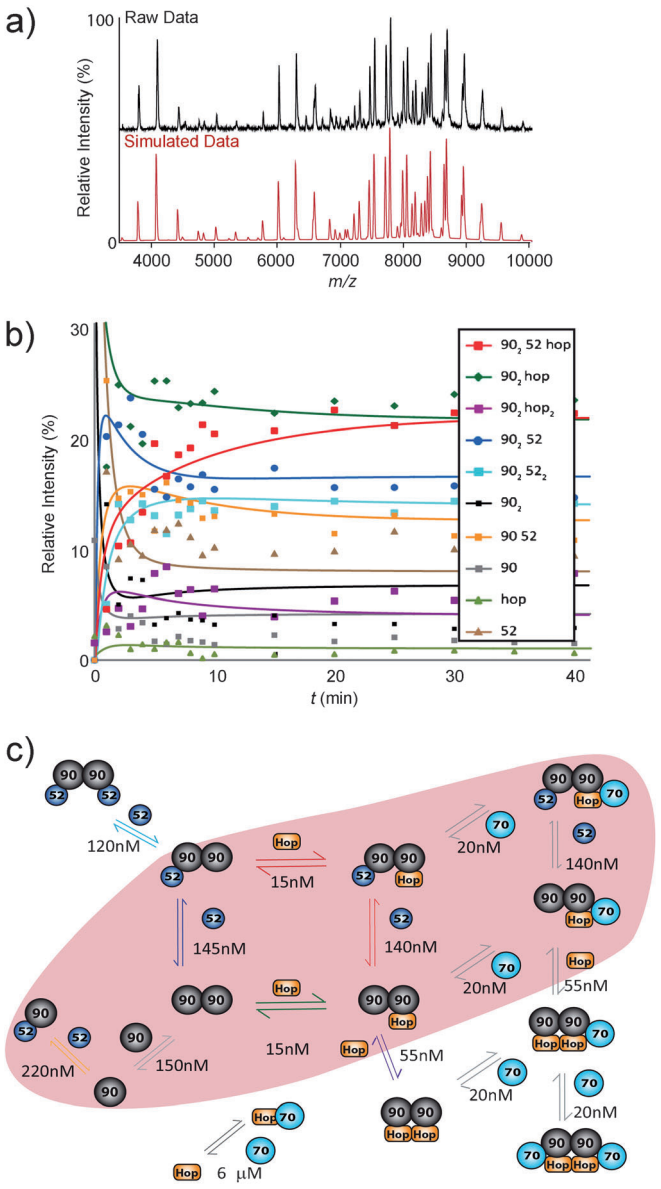

Figure 4. The deconvolution of multiple coexisting species is achieved using in-house software (Massign).[57] a) The mass spectrum (red) represents the sum of the simulations of the individual mass spectra of all component complexes, which aids the assignment of experimental data (black). The intensities of each component are adjusted to simulate the raw data. b) Time course data for the population of ten complexes formed en route to equilibrium in solution. K_D values were calculated, and a network of all possible complexes formed was constructed. c) Overview of the interactions observed between HSP90 (gray), FKBP52 (purple), Hop (orange), and HSP70 (blue). Complexes highlighted in red are those that are likely to form at cellular concentrations. K_D values are given next to the reaction arrows. Figure adapted from Ref. [29].

lian complexes were shown to exchange monomeric subunits, indicating that the polydispersity of αB-crystallin can be understood by studying the interactions between monomers within the dimeric building blocks of the assembly.[16b] To increase the throughput of these subunit exchange experiments, two sHSPs from *Arabidopsis thaliana* were studied using an automated chip-based nESI source.[66] Subunit exchange experiments revealed that the intradimeric building blocks were interchanged between the oligomers, hence the most prominent oligomers observed were composed of an even number of subunits (Figure 5). The rate constants observed for these complexes were also in agreement to those obtained for other plant sHSPs, which were obtained using an MS approach.[67]

Capturing dynamic regions is often the most challenging task of structural biology but interestingly, these are often readily accessible by MS. In the case of the ribosome, the stalk complexes, which are the flexible, five-protein protuberances on the ribosome, are frequently absent in high-resolution X-ray structures but are readily observed by MS.[68] These stalk complexes play a key role in function as they are responsible for the interactions formed with translation factors during protein biosynthesis.[69] The stalk complex of *E. coli* ribosomes consists of one copy of the L10 protein and four copies of the L7/L12 proteins. The exchange kinetics of the stalk complex were investigated in a real-time reaction monitoring experiment using isotopically labelled L7/L12, while the stalk was still associated with the intact ribosome.[70] The MS data revealed the independent nature of the L7–L12 dimers, which appeared to associate and dissociate as readily as the individual monomers. In ribosome EF-G complexes, where the ribosome is trapped in a post-translational state, it was demonstrated that one of the L7–L12 dimers became trapped on the ribosome. This results in a 27 % lower rate of monomer disassembly and a 47 % reduction in dimer exchange, clearly demonstrating a preference for interactions of the L7–L12 dimers with elongation factors.

Relating quaternary dynamics to disease states is illustrated in studies of tetrameric transthyretin, an amyloidogenic protein, mutations of which are implicated in the development of familial amyloidotic polyneuropathy.[71] One of the most common amyloidogenic mutations identified is L55P.[71c] Subunit exchange in a tetrameric L55P variant was compared to that in the wild-type (WT) protein.[72] Although the WT protein was shown to exchange via both monomers and dimers, the disease mutant primarily interchanges by dimeric subunits. The two dissociation events were combined to provide overall rate constants of 0.017 min^{-1} and 0.0011 min^{-1} for the L55P variant and the wild-type protein, respectively. Most interestingly, the rate of dissociation in WT transthyretin is increased in the presence of L55P. As the tetrameric complex does not proceed to form fibrils, it was concluded that the interaction between the WT and the mutant could promote the formation of insoluble aggregates by increasing the amount of dissociation products of the WT form. This has implications for heterozygotes expressing both proteins; interactions between tetramers during their lifetime in plasma (half-life 8–18 h) could help explain the amyloidogenicity of the L55P variant.

In analogous experiments targeting β_2-microglobulin (β_2m), which has been identified as the major component of amyloid fibrils associated with dialysis-related amyloidosis,[16a] real-time ESI–IM–MS measurements were used to monitor the subunit exchange of ^{14}N- and ^{15}N-labelled prefibrillar oligomers of β_2m. These early oligomers were shown to be dynamic, with the rate of subunit exchange decreasing

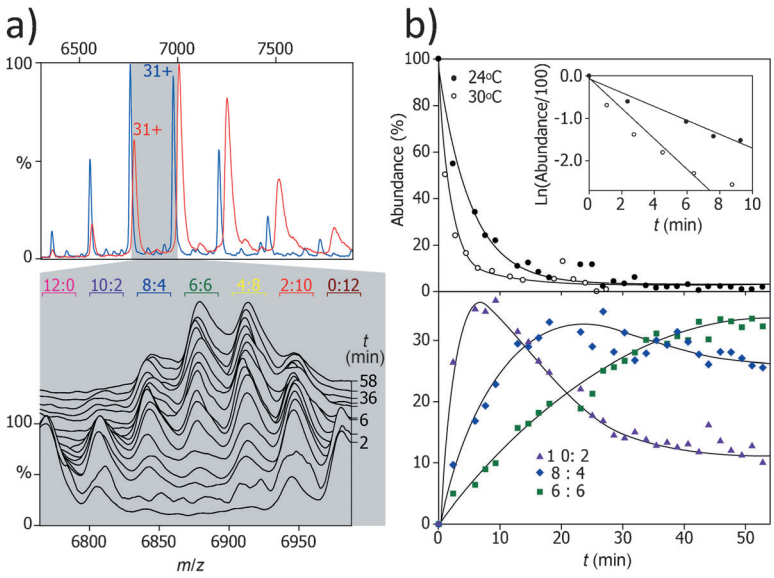

Figure 5. The subunit exchange between HSP17.6 (red) and HSP18.1 (blue) from *Arabidopsis thaliana*. a) Mass spectra of the two proteins illustrate the ability to resolve the two complexes by mass. With time, these discrete peaks are replaced by new species that form with a range of stoichiometries consistent with the exchange of dimers between the two assemblies (lower panel). b) Exponential decay of the homododecamers at 30 °C (white circles) and at 24 °C (black circles). The relative abundances of heterododecamers 10:2 (purple triangles), 8:4 (blue diamonds), and 6:6 (green squares) illustrate that exchange proceeds via dimers (lower panel). Figure adapted from Ref. [66].

with increasing oligomeric size. By monitoring the dynamics of these early oligomers, as well as obtaining structural information from IM measurements, the authors were able to construct a model of the early oligomer assembly of this protein.

8. First Applications to Membrane Proteins

The ability to study intact membrane proteins in the gas phase is a recent achievement that expands the application of the technique to some of the most challenging complexes in structural biology.[73] Based on their low expression levels and solubility issues, a growing but relatively limited number of structures have been solved at atomic resolution. The MS approach involves introducing membrane proteins encapsulated in detergent micelles from charged droplets, and subsequently releasing naked protein assemblies by applying collisional activation.[73c] The ability to preserve protein–protein interactions, including those between transmembrane subunits, was established, but whether interactions with small ligands could be preserved was less clear at that time. This was particularly challenging given the presence of the detergent micelle, which has to be removed while small molecule ligand binding needs to be retained.

The integral membrane protein P-glycoprotein (P-gp)[74] is an ATP-binding cassette (ABC) transporter that is responsible for pumping a variety of substrates across the membrane and has been subjected to X-ray analysis.[75] Because of its ability to pump substrates, P-gp is implicated in multidrug resistance, acting as an efflux pump that ejects chemotherapeutics from target cancer cells.[76] P-gp contains two transmembrane regions, each containing six transmembrane helices.[75,77] These helices form a hydrophobic binding cavity, within which the substrate resides. An ATP-driven conformational rearrangement is proposed to eject the substrate to the opposing side of the membrane (Figure 6a).[78] Time-resolved measurements were used to monitor the intensity of various species with lipid bound species, enabling the calculation of K_D values (Figure 6c).[74] Results revealed that up to six negatively charged lipids are able to bind simultaneously to P-gp, more favorably than zwitterionic lipids (Figure 6b). Ion mobility measurements illustrate that the protein exists in a delicate equilibrium between two conformations, which were assigned to inward- and outward-facing forms. The addition of ligands and lipids appears to stabilize the smaller, outward-facing conformer, which is required for efflux (Figure 6d). Previous studies performed on P-gp, which were designed to monitor conformational dynamics, included FRET[78] and EPR experiments.[79] In contrast, these MS studies were performed using unlabeled protein/ligands and were able to monitor simultaneously the conformational changes induced by multiple binding partners. Unexpectedly, the binding of cyclosporine A (CsA) was found to enhance the binding of cardiolipin, leading to the proposal that CsA stabilizes an open conformation and subsequently improves access of cardiolipin to the internal binding cavity.

Protein complexes that consist of soluble proteins and multiple membrane-embedded subcomplexes are a particular challenge for all structural techniques. This architecture is exemplified by the complexes formed by the colicins, cytotoxic proteins expressed and released by *E. coli*, which kill other closely related bacteria during interbacterial competition. Colicin E9 (ColE9) initially anchors to the vitamin B_{12} receptor BtuB, before recruiting the trimeric membrane porin OmpF through the intrinsically disordered N-terminus ColE9. This intrinsically disordered domain of ColE9 passes through one of the three porins of OmpF and captures the periplasmic protein TolB on the other side of the membrane (Figure 7a, inset). A disulfide trap between ColE9 and TolB allowed the extraction and purification of the full heptameric protein assembly using a detergent to protect transmembrane protein subunits in two different membrane-embedded locations. This assembly is therefore likely extracted in two detergent micelles; however, by carefully controlled acceleration to remove the detergent, the intact complex of approximately 300 kDa was liberated in the gas phase confirming the stoichiometry of the assembly (Figure 7a). The release of this complex from two micelles is in line with recent proposals of a protective role of detergent evaporation in maintaining membrane protein complexes in the gas phase.[80]

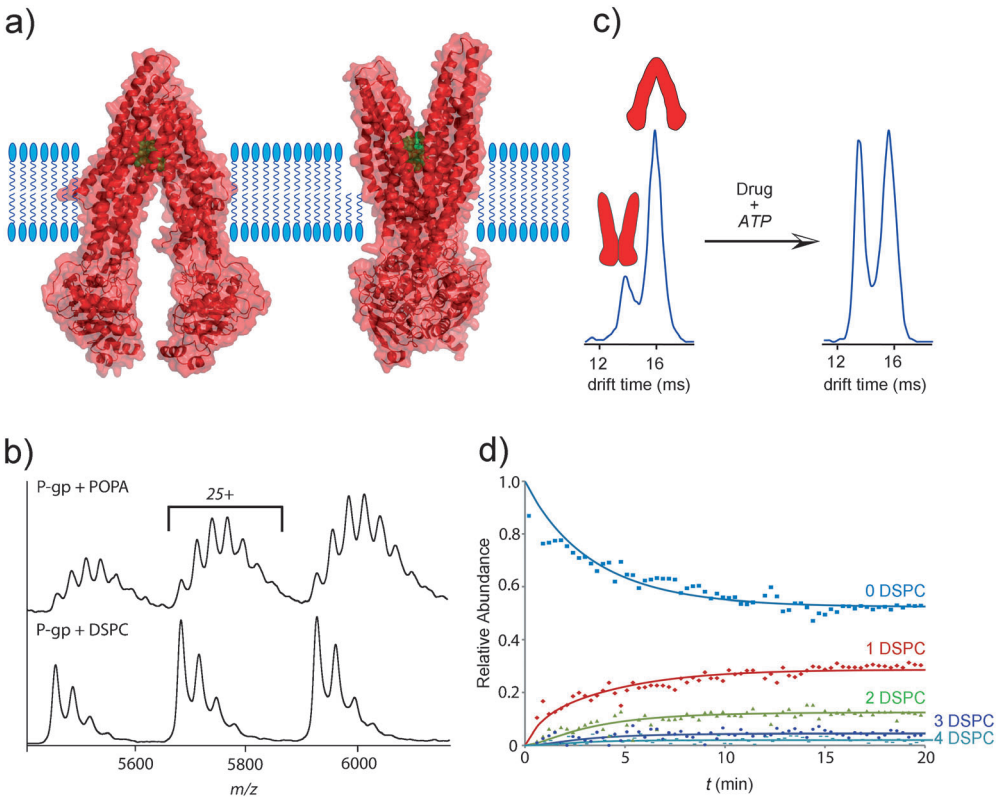

Figure 6. a) PgP undergoes conformational transitions to accomplish transport across the membrane. b) The preference towards negatively charged lipids is demonstrated by observing additional peaks that correspond to binding of up to six POPA lipids, compared to the binding of a maximum of three 1,2-distearoyl-*sn*-glycero-3-phosphocholine (DSPC) when added to P-gp in detergent micelles. c) The IM–MS data reveal two conformational states, which were assigned to the open and closed states of the protein, the equilibrium of which is affected by drug, detergent, and ATP binding. d) The kinetics of lipid binding can be monitored by recording spectra at specific time points, and fitting the data allows the association rates to be determined.

A proteolyzed fragment of the full translocon, which still retains an active OmpF trimer, allowed the determination of the interaction of the OmpF binding epitope of colicin (Figure 7b). A K_D value of 1.4 μM was determined through concentration-controlled addition of a peptide that replicates the OmpF binding epitope of ColE9. This K_D value is in good agreement with a subsequent ITC measurement performed in the same buffer ($K_D = 1$ μM; Figure 7b–d). This MS study therefore revealed that reliable K_D measurements can be made for membrane complexes and moreover showed from the stoichiometry of the peptide binding that only one of the OmpF porins was accessible for peptide binding in the presence of ColE9. A confirmation of this hypothesis, which was provided by electron microscopy (EM) and electrical conductivity measurements, allowed a new signaling mechanism to be proposed, whereby the colicin enters the periplasm and threads back through a vacant porin. Anchoring this intrinsically disordered domain by two pores is thought to lower the entropic penalty for the epitope exposed at the periplasm side to bind to its TolB target.

9. Summary and Outlook

In this Review, we have highlighted some of the unique insights provided when using MS approaches to study interactions within protein complexes. The power of the approach derives from its ability to follow and simultaneously observe complex interaction cascades that take place in solution. This alleviates the need to study interactions in isolation and enables their study within a homogeneous preparation, as illustrated for the HSP90 reaction cycle. The time scale of the MS approach also enables studies in real time. Where complexes are present as polydisperse oligomeric assemblies, MS presents an exclusive opportunity to study the effects of subunit dynamics on the structure, which in turn can be related to their function.

Extracting quantitative affinity data for membrane complexes, which was highlighted for the colicin translocon and PgP complexes, represents some of the first examples where K_D measurements have been made for membrane protein complexes and paves the way for many follow-up studies. New approaches have recently been developed for studying membrane proteins from lipid-bilayer environments.[81] A particularly novel application of solubilized bilayers, in the context of this Review, is the ability to monitor the interactions between soluble proteins and nanodiscs containing specific glycosphingolipids (GSL).[82] Together, these developments highlight opportunities for quantifying native-like binding interactions between proteins and lipids that have been attained to date for complexes released from detergent micelles.

In this Review, we have shown how MS has progressed to obtain numerical values for reaction rates and binding constants, overcoming many of the initial challenges, including non-specific binding, preservation of hydrophobic interactions, and unwanted dissociation. Often acceptance of quantitative data deduced by MS requires validation with other approaches carried out in parallel. Although a multifaceted approach is always desirable, and to this end, closely linking MS with ITC, EM, and X-ray analysis is of paramount importance, affinities can now be deduced ab initio by means of MS. As we move into a new era for MS of membrane

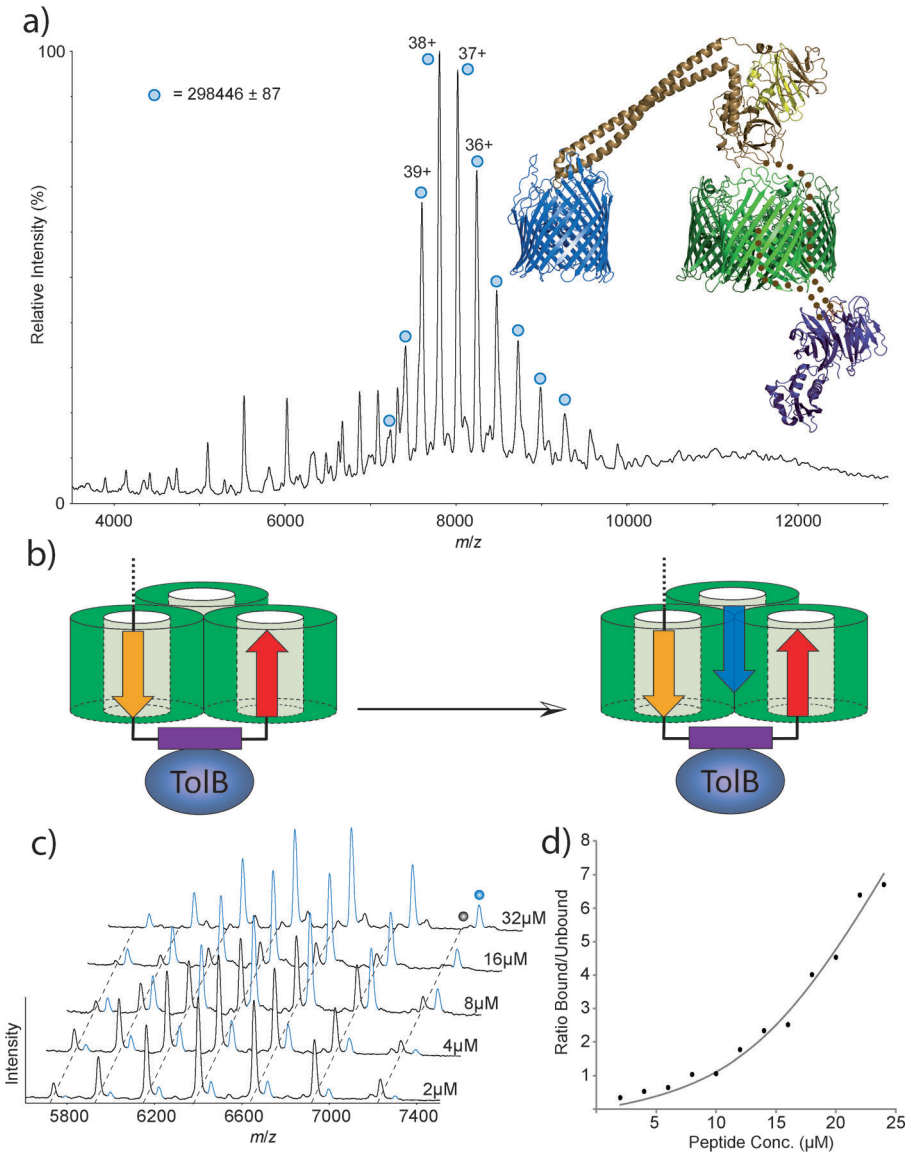

Figure 7. a) Mass spectrum of the complete transmembrane translocon (blue circles) released from two detergent micelles. b, c) Adding increasing concentrations of a peptide that replicates the OmpF binding epitope of ColE9 to the proteolyzed translocon fragment reveals that only one porin remains unoccupied. d) Affinity data for the OmpF–peptide interactions was calculated in excellent agreement with the ITC results.

proteins, megadalton viruses, nanodiscs, and dynamic reaction cycles, it is interesting to consider the likely impact of new developments in instrumentation. In this regard, the ability to increase mass resolution using new Orbitrap modifications,[83] to map non-covalent binding sites with electron-capture dissociation,[84] to enhance separation in ion mobility measurements,[85] and to link MS more closely with EM[86] looks set to augment this burgeoning research area for many years to come.

We are extremely grateful to Julien Marcoux, Justin Benesch, Michal Sharon, Stephen Ambrose, Kallol Gupta, Ima-obong Ebong, Nicholas Housden, Carla Schmidt, Joseph Gault, and Neil Oldham for helpful advice and donation of figures. J.T.S.H. is funded by a Medical Research Council Programme Grant to C.V.R. (98101), and C.V.R. is funded by an ERC grant ("IMPRESS", 26851) and a Royal Society Professorship.

Received: March 26, 2014
Published online: October 29, 2014

[1] A. C. Gingras, M. Gstaiger, B. Raught, R. Aebersold, *Nat. Rev. Mol. Cell Biol.* **2007**, *8*, 645–654.
[2] G. W. Li, X. S. Xie, *Nature* **2011**, *475*, 308–315.
[3] H. Kitano, *Science* **2002**, *295*, 1662–1664.
[4] K. Vuignier, J. Schappler, J.-L. Veuthey, P.-A. Carrupt, S. Martel, *Anal. Bioanal. Chem.* **2010**, *398*, 53–66.
[5] D. S. Hage, S. A. Tweed, *J. Chromatogr. B* **1997**, *699*, 499–525.
[6] N. H. H. Heegaard, R. T. Kennedy, *Electrophoresis* **1999**, *20*, 3122–3133.
[7] J. Fenn, M. Mann, C. Meng, S. Wong, C. Whitehouse, *Science* **1989**, *246*, 64–71.
[8] M. Karas, U. Bahr, T. Dulcks, *Fresenius J. Anal. Chem.* **2000**, *366*, 669–676.
[9] a) J. T. S. Hopper, A. Rawlings, J. P. Afonso, D. Channing, R. Layfield, N. J. Oldham, *J. Am. Soc. Mass Spectrom.* **2012**, *23*, 1757–1767; b) B. Ganem, Y. T. Li, J. D. Henion, *J. Am. Chem. Soc.* **1991**, *113*, 6294–6296; c) V. Katta, B. T. Chait, *J. Am. Chem. Soc.* **1991**, *113*, 8534–8535.
[10] F. Sobott, H. Hernandez, M. G. McCammon, M. A. Tito, C. V. Robinson, *Anal. Chem.* **2002**, *74*, 1402–1407.
[11] a) J. L. P. Benesch, B. T. Ruotolo, D. A. Simmons, C. V. Robinson, *Chem. Rev.* **2007**, *107*, 3544–3567; b) I. V. Chernushevich, B. A. Thomson, *Anal. Chem.* **2004**, *76*, 1754–1760; c) N. Tahallah, M. Pinkse, C. S. Maier, A. J. Heck, *Rapid Commun. Mass Spectrom.* **2001**, *15*, 596–601; d) R. H. H. van den Heuvel, E. van Duijn, H. Mazon, S. A. Synowsky, K. Lorenzen, C. Versluis, S. J. J. Brouns, D. Langridge, J. van der Oost, J. Hoyes, A. J. R. Heck, *Anal. Chem.* **2006**, *78*, 7473–7483.
[12] A. R. McKay, B. T. Ruotolo, L. L. Ilag, C. V. Robinson, *J. Am. Chem. Soc.* **2006**, *128*, 11433–11442.
[13] M. Sharon, S. Witt, E. Glasmacher, W. Baumeister, C. V. Robinson, *J. Biol. Chem.* **2007**, *282*, 18448–18457.
[14] J. Snijder, R. J. Rose, D. Veesler, J. E. Johnson, A. J. Heck, *Angew. Chem.* **2013**, *125*, 4112–4115; *Angew. Chem. Int. Ed.* **2013**, *52*, 4020–4023.
[15] a) J. A. Loo, *Mass Spectrom. Rev.* **1997**, *16*, 1–23; b) C. Uetrecht, A. J. R. Heck, *Angew. Chem.* **2011**, *123*, 8398–8413; *Angew. Chem. Int. Ed.* **2011**, *50*, 8248–8262.

[16] a) D. P. Smith, S. E. Radford, A. E. Ashcroft, *Proc. Natl. Acad. Sci. USA* **2010**, *107*, 6794 – 6798; b) A. J. Baldwin, H. Lioe, C. V. Robinson, L. E. Kay, J. L. P. Benesch, *J. Mol. Biol.* **2011**, *413*, 297 – 309.

[17] J. J. Sims, A. Haririnia, B. C. Dickinson, D. Fushman, R. E. Cohen, *Nat. Struct. Mol. Biol.* **2009**, *16*, 883-U112.

[18] a) Z. Hall, C. V. Robinson, *J. Am. Soc. Mass Spectrom.* **2012**, *23*, 1161 – 1168; b) I. A. Kaltashov, A. Mohimen, *Anal. Chem.* **2005**, *77*, 5370 – 5379.

[19] E. N. Kitova, A. El-Hawiet, P. D. Schnier, J. S. Klassen, *J. Am. Soc. Mass Spectrom.* **2012**, *23*, 431 – 441.

[20] J. M. Daniel, S. D. Friess, S. Rajagopalan, S. Wendt, R. Zenobi, *Int. J. Mass Spectrom.* **2002**, *216*, 1 – 27.

[21] L. Liu, E. N. Kitova, J. S. Klassen, *J. Am. Soc. Mass Spectrom.* **2011**, *22*, 310 – 318.

[22] a) L. Han, E. N. Kitova, M. Tan, X. Jiang, J. S. Klassen, *J. Am. Soc. Mass Spectrom.* **2014**, *25*, 111 – 119; b) H. Lin, E. N. Kitova, J. S. Klassen, *J. Am. Soc. Mass Spectrom.* **2014**, *25*, 104 – 110; c) Y. Z. Liu, B. Su, X. Wang, *Rapid Commun. Mass Spectrom.* **2012**, *26*, 719 – 727.

[23] a) P. W. Huang, T. Farkas, S. Marionneau, W. M. Zhong, N. Ruvoen-Clouet, A. L. Morrow, M. Altaye, L. K. Pickering, D. S. Newburg, J. LePendu, X. Jiang, *J. Infect. Dis.* **2003**, *188*, 19 – 31; b) P. W. Huang, T. Farkas, W. M. Zhong, S. Thornton, A. L. Morrow, J. Xi, *J. Virol.* **2005**, *79*, 6714 – 6722.

[24] L. Han, P. I. Kitov, E. N. Kitova, M. Tan, L. Y. Wang, M. Xia, X. Jiang, J. S. Klassen, *Glycobiology* **2013**, *23*, 276 – 285.

[25] A. El-Hawiet, E. N. Kitova, D. Arutyunov, D. J. Simpson, C. M. Szymanski, J. S. Klassen, *Anal. Chem.* **2012**, *84*, 3867 – 3870.

[26] A. El-Hawiet, G. K. Shoemaker, R. Daneshfar, E. N. Kitova, J. S. Klassen, *Anal. Chem.* **2012**, *84*, 50 – 58.

[27] a) B. T. Ruotolo, K. Giles, I. Campuzano, A. M. Sandercock, R. H. Bateman, C. V. Robinson, *Science* **2005**, *310*, 1658 – 1661; b) C. Uetrecht, R. J. Rose, E. van Duijn, K. Lorenzen, A. J. R. Heck, *Chem. Soc. Rev.* **2010**, *39*, 1633 – 1655.

[28] A. El-Hawiet, E. N. Kitova, J. S. Klassen, *Anal. Chem.* **2013**, *85*, 7637 – 7644.

[29] I.-o. Ebong, N. Morgner, M. Zhou, M. A. Saraiva, S. Daturpalli, S. E. Jackson, C. V. Robinson, *Proc. Natl. Acad. Sci. USA* **2011**, *108*, 17939 – 17944.

[30] L. Konermann, B. A. Collings, D. J. Douglas, *Biochemistry* **1997**, *36*, 5554 – 5559.

[31] a) L. Konermann, F. I. Rosell, A. G. Mauk, D. J. Douglas, *Biochemistry* **1997**, *36*, 6448 – 6454; b) L. Konermann, D. J. Douglas, *Rapid Commun. Mass Spectrom.* **1998**, *12*, 435 – 442; c) Y. L. Chen, J. M. Campbell, B. A. Collings, L. Konermann, D. J. Douglas, *Rapid Commun. Mass Spectrom.* **1998**, *12*, 1003 – 1010.

[32] J. Liu, L. Konermann, *Biochemistry* **2013**, *52*, 1717 – 1724.

[33] Z. L. Li, A. K. Sau, S. D. Shen, C. Whitehouse, T. Baasov, K. S. Anderson, *J. Am. Chem. Soc.* **2003**, *125*, 9938 – 9939.

[34] Z. Miao, H. Chen, P. Liu, Y. Liu, *Anal. Chem.* **2011**, *83*, 3994 – 3997.

[35] M. Peschke, U. H. Verkerk, P. Kebarle, *J. Am. Soc. Mass Spectrom.* **2004**, *15*, 1424 – 1434.

[36] L. Konermann, E. Ahadi, A. D. Rodriguez, S. Vahidi, *Anal. Chem.* **2013**, *85*, 2 – 9.

[37] J. L. P. Benesch, B. T. Ruotolo, *Curr. Opin. Struct. Biol.* **2011**, *21*, 641 – 649.

[38] a) L. Shimon, M. Sharon, A. Horovitz, *Biophys. J.* **2010**, *99*, 1645 – 1649; b) L. A. Lane, B. T. Ruotolo, C. V. Robinson, G. Favrin, J. L. P. Benesch, *Int. J. Mass Spectrom.* **2009**, *283*, 169 – 177.

[39] J. X. Sun, E. N. Kitova, W. J. Wang, J. S. Klassen, *Anal. Chem.* **2006**, *78*, 3010 – 3018.

[40] H. Lin, E. N. Kitova, J. S. Klassen, *Anal. Chem.* **2013**, *85*, 8919 – 8922.

[41] K. Sokratous, L. V. Roach, D. Channing, J. Strachan, J. Long, M. S. Searle, R. Layfield, N. J. Oldham, *J. Am. Chem. Soc.* **2012**, *134*, 6416 – 6424.

[42] J. L. P. Benesch, C. V. Robinson, *Nature* **2009**, *462*, 576 – 577.

[43] a) J. Sun, E. N. Kitova, J. S. Klassen, *Anal. Chem.* **2007**, *79*, 416 – 425; b) D. Cubrilovic, A. Biela, F. Sielaff, T. Steinmetzer, G. Klebe, R. Zenobi, *J. Am. Soc. Mass Spectrom.* **2012**, *23*, 1768 – 1777.

[44] a) J. T. S. Hopper, K. Sokratous, N. J. Oldham, *Anal. Biochem.* **2012**, *421*, 788 – 790; b) G. R. Hilton, G. K. Hochberg, A. Laganowsky, S. I. McGinnigle, A. J. Baldwin, J. L. Benesch, *Philos. Trans. R. Soc. London Ser. B* **2013**, *368*, 20110405; c) J. T. S. Hopper, N. J. Oldham, *Anal. Chem.* **2011**, *83*, 7472 – 7479.

[45] J. Marcoux, C. V. Robinson, *Structure* **2013**, *21*, 1541 – 1550.

[46] a) R. Franski, B. Gierczyk, T. Kozik, *Rapid Commun. Mass Spectrom.* **2008**, *22*, 2747 – 2749; b) V. Gabelica, N. Galic, E. De Pauw, *J. Am. Soc. Mass Spectrom.* **2002**, *13*, 946 – 953; c) B. Kralj, A. Smidovnik, J. Kobe, *Rapid Commun. Mass Spectrom.* **2009**, *23*, 171 – 180.

[47] a) L. Liu, D. Bagal, E. N. Kitova, P. D. Schnier, J. S. Klassen, *J. Am. Chem. Soc.* **2009**, *131*, 15980 – 15981; b) L. Liu, K. Michelsen, E. N. Kitova, P. D. Schnier, J. S. Klassen, *J. Am. Chem. Soc.* **2010**, *132*, 17658 – 17660.

[48] K. Barylyuk, R. M. Balabin, D. Gruenstein, R. Kikkeri, V. Frankevich, P. H. Seeberger, R. Zenobi, *J. Am. Soc. Mass Spectrom.* **2011**, *22*, 1167 – 1177.

[49] K. Breuker, F. W. McLafferty, *Proc. Natl. Acad. Sci. USA* **2008**, *105*, 18145 – 18152.

[50] J. Kuriyan, D. Eisenberg, *Nature* **2007**, *450*, 983 – 990.

[51] a) W. Chazin, T. D. Veenstra, *Rapid Commun. Mass Spectrom.* **1999**, *13*, 548 – 555; b) P. M. Gehrig, C. H. You, R. Dallinger, C. Gruber, M. Brouwer, J. H. R. Kagi, P. E. Hunziker, *Protein Sci.* **2000**, *9*, 395 – 402.

[52] H. Rogniaux, S. Sanglier, K. Strupat, S. Azza, O. Roitel, V. Ball, D. Tritsch, G. Branlant, A. Van Dorsselaer, *Anal. Biochem.* **2001**, *291*, 48 – 61.

[53] D. Cubrilovic, W. Haap, K. Barylyuk, A. Ruf, M. Badertscher, M. Gubler, T. Tetaz, C. Joseph, J. Benz, R. Zenobi, *ACS Chem. Biol.* **2014**, *9*, 218 – 226.

[54] A. Dyachenko, R. Gruber, L. Shimon, A. Horovitz, M. Sharon, *Proc. Natl. Acad. Sci. USA* **2013**, *110*, 7235 – 7239.

[55] A. Horovitz, K. R. Willison, *Curr. Opin. Struct. Biol.* **2005**, *15*, 646 – 651.

[56] D. Picard, *Cell. Mol. Life Sci.* **2002**, *59*, 1640 – 1648.

[57] N. Morgner, C. V. Robinson, *Anal. Chem.* **2012**, *84*, 2939 – 2948.

[58] R. J. Rose, A. F. Labrijn, E. T. J. van den Bremer, S. Loverix, I. Lasters, P. H. C. van Berkel, J. G. J. van de Winkel, J. Schuurman, P. W. H. I. Parren, A. J. R. Heck, *Structure* **2011**, *19*, 1274 – 1282.

[59] C. Uetrecht, N. R. Watts, S. J. Stahl, P. T. Wingfield, A. C. Steven, A. J. R. Heck, *Phys. Chem. Chem. Phys.* **2010**, *12*, 13368 – 13371.

[60] S. Kang, L. M. Oltrogge, C. C. Broomell, L. O. Liepold, P. E. Prevelige, M. Young, T. Douglas, *J. Am. Chem. Soc.* **2008**, *130*, 16527 – 16529.

[61] M. Haslbeck, T. Franzmann, D. Weinfurtner, J. Buchner, *Nat. Struct. Mol. Biol.* **2005**, *12*, 842 – 846.

[62] a) J. Horwitz, *Proc. Natl. Acad. Sci. USA* **1992**, *89*, 10449 – 10453; b) J. P. Brady, D. Garland, Y. Duglas-Tabor, W. G. Robison, A. Groome, E. F. Wawrousek, *Proc. Natl. Acad. Sci. USA* **1997**, *94*, 884 – 889.

[63] H. Ecroyd, J. A. Carver, *Cell. Mol. Life Sci.* **2009**, *66*, 62 – 81.

[64] J. Horwitz, *Semin. Cell Dev. Biol.* **2000**, *11*, 53 – 60.

[65] J. A. Aquilina, J. L. P. Benesch, L. L. Ding, O. Yaron, J. Horwitz, C. V. Robinson, *J. Biol. Chem.* **2005**, *280*, 14485 – 14491.

[66] A. J. Painter, N. Jaya, E. Basha, E. Vierling, C. V. Robinson, J. L. P. Benesch, *Chem. Biol.* **2008**, *15*, 246 – 253.

[67] F. Sobott, J. L. P. Benesch, E. Vierling, C. V. Robinson, *J. Biol. Chem.* **2002**, *277*, 38921 – 38929.
[68] a) L. L. Ilag, H. Videler, A. R. McKay, F. Sobott, P. Fucini, K. H. Nierhaus, C. V. Robinson, *Proc. Natl. Acad. Sci. USA* **2005**, *102*, 8192 – 8197; b) C. L. Hanson, H. Videler, C. Santos, J. P. G. Ballesta, C. V. Robinson, *J. Biol. Chem.* **2004**, *279*, 42750 – 42757.
[69] A. A. D. Beauclerk, E. Cundliffe, J. Dijk, *J. Biol. Chem.* **1984**, *259*, 6559 – 6563.
[70] S. Deroo, S.-J. Hyung, J. Marcoux, Y. Gordiyenko, R. K. Koripella, S. Sanyal, C. V. Robinson, *ACS Chem. Biol.* **2012**, *7*, 1120 – 1127.
[71] a) M. J. M. Saraiva, *Hum. Mutat.* **1995**, *5*, 191 – 196; b) V. Plante-Bordeneuve, T. Lalu, M. Misrahi, M. M. Reilly, D. Adams, C. Lacroix, G. Said, *Neurology* **1998**, *51*, 708 – 714; c) Y. Sekijima, R. L. Wiseman, J. Matteson, P. Hammarstrom, S. R. Miller, A. R. Sawkar, W. E. Balch, J. W. Kelly, *Cell* **2005**, *121*, 73 – 85.
[72] C. A. Keetch, E. H. C. Bromley, M. G. McCammon, N. Wang, J. Christodoulou, C. V. Robinson, *J. Biol. Chem.* **2005**, *280*, 41667 – 41674.
[73] a) N. P. Barrera, N. Di Bartolo, P. J. Booth, C. V. Robinson, *Science* **2008**, *321*, 243 – 246; b) N. P. Barrera, C. V. Robinson, *Annu. Rev. Biochem.* **2011**, *80*, 247 – 271; c) A. Laganowsky, E. Reading, J. T. Hopper, C. V. Robinson, *Nat. Protoc.* **2013**, *8*, 639 – 651.
[74] J. Marcoux, S. C. Wang, A. Politis, E. Reading, J. Ma, P. C. Biggin, M. Zhou, H. Tao, Q. Zhang, G. Chang, N. Morgner, C. V. Robinson, *Proc. Natl. Acad. Sci. USA* **2013**, *110*, 9704 – 9709.
[75] R. J. Dawson, K. P. Locher, *Nature* **2006**, *443*, 180 – 185.
[76] G. Szakács, J. K. Paterson, J. A. Ludwig, C. Booth-Genthe, M. M. Gottesman, *Nat. Rev. Drug Discovery* **2006**, *5*, 219 – 234.
[77] S. G. Aller, J. Yu, A. Ward, Y. Weng, S. Chittaboina, R. Zhuo, P. M. Harrell, Y. T. Trinh, Q. Zhang, I. L. Urbatsch, G. Chang, *Science* **2009**, *323*, 1718 – 1722.
[78] B. Verhalen, S. Ernst, M. Borsch, S. Wilkens, *J. Biol. Chem.* **2012**, *287*, 1112 – 1127.
[79] a) I. Hänelt, D. Wunnicke, E. Bordignon, H.-J. Steinhoff, D. J. Slotboom, *Nat. Struct. Mol. Biol.* **2013**, *20*, 210 – 214; b) E. R. Georgieva, P. P. Borbat, C. Ginter, J. H. Freed, O. Boudker, *Nat. Struct. Mol. Biol.* **2013**, *20*, 215 – 221.
[80] a) A. J. Borysik, D. J. Hewitt, C. V. Robinson, *J. Am. Chem. Soc.* **2013**, *135*, 6078 – 6083; b) S. C. Wang, A. Politis, N. Di Bartolo, V. N. Bavro, S. J. Tucker, P. J. Booth, N. P. Barrera, C. V. Robinson, *J. Am. Chem. Soc.* **2010**, *132*, 15468 – 15470.
[81] a) M. T. Marty, H. Zhang, W. Cui, M. L. Gross, S. G. Sligar, *J. Am. Soc. Mass Spectrom.* **2013**, *25*, 269 – 277; b) J. T. S. Hopper, Y. T.-C. Yu, D. Li, A. Raymond, M. Bostock, I. Liko, V. Mikhailov, A. Laganowsky, J. L. P. Benesch, M. Caffrey, D. Nietlispach, C. V. Robinson, *Nat. Methods* **2013**, *10*, 1206 – 1208.
[82] Y. X. Zhang, L. Liu, R. Daneshfar, E. N. Kitova, C. S. Li, F. Jia, C. W. Cairo, J. S. Klassen, *Anal. Chem.* **2012**, *84*, 7618 – 7621.
[83] R. J. Rose, E. Damoc, E. Denisov, A. Makarov, A. J. R. Heck, *Nat. Methods* **2012**, *9*, 1084 – 1086.
[84] a) Y. Xie, J. Zhang, S. Yin, J. A. Loo, *J. Am. Chem. Soc.* **2006**, *128*, 14432 – 14433; b) H. Zhang, W. Cui, J. Wen, R. E. Blankenship, M. L. Gross, *Anal. Chem.* **2011**, *83*, 5598 – 5606.
[85] a) K. Giles, J. P. Williams, I. Campuzano, *Rapid Commun. Mass Spectrom.* **2011**, *25*, 1559 – 1566; b) S. I. Merenbloom, R. S. Glaskin, Z. B. Henson, D. E. Clemmer, *Anal. Chem.* **2009**, *81*, 1482 – 1487.
[86] J. L. P. Benesch, B. T. Ruotolo, D. A. Simmons, N. P. Barrera, N. Morgner, L. C. Wang, R. Helen, C. V. Robinson, *J. Struct. Biol.* **2010**, *172*, 161 – 168.